Precision Timing Detectors with Cadmium Telluride Sensor

A. Bornheim[a], C. Pena[a], M. Spiropulu[a], S. Xie[*,a], Z. Zhang[a]

[a] *California Institute of Technology, Pasadena, CA, USA*

Abstract

Precision timing detectors for high energy physics experiments with temporal resolutions of a few 10 ps are of pivotal importance to master the challenges posed by the highest energy particle accelerators such as the LHC. Calorimetric timing measurements have been a focus of recent research, enabled by exploiting the temporal coherence of electromagnetic showers. Scintillating crystals with high light yield as well as silicon sensors are viable sensitive materials for sampling calorimeters. Silicon sensors have very high efficiency for charged particles. However, their sensitivity to photons, which comprise a large fraction of the electromagnetic shower, is limited. A large fraction of the energy in an electromagnetic shower is carried by photons. To enhance the efficiency of detecting photons, materials with higher atomic numbers than silicon are preferable. In this paper we present test beam measurements with a Cadmium-Telluride sensor as the active element of a secondary emission calorimeter with focus on the timing performance of the detector. A Schottky type Cadmium-Telluride sensor with an active area of 1 cm^2 and a thickness of 1 mm is used in an arrangement with tungsten and lead absorbers. Measurements are performed with electron beams in the energy range from 2 GeV to 200 GeV. A timing resolution of 25 ps is achieved under the best conditions.

Key words: Cadmium Telluride, Timing, Calorimeter

1. Introduction

There has been much recent interest in highly granular calorimeters with precision timing capability at the level of $20-30$ ps in light of the High-Luminosity LHC and future higher energy hadron colliders. In order to probe increasingly rare interactions, future hadron colliders must provide large instantaneous luminosity well above 10^{35} $cm^{-2}s^{-1}$. With current accelerator and particle detector capabilities, such a high instantaneous luminosity will result in very large amounts of pileup, exceeding several hundreds of simultaneous inelastic collisions per bunch crossing. Therefore, the crucial ability to identify the origin of the particles produced at the different interaction points will be severely degraded. Precision timing detectors can be used to recover the ability to discriminate between particles produced by different inelastic collisions [1]. For beam bunch profiles similar to that of the LHC, a detector that can measure the time of arrival of a

*Corresponding author
Email address: sixie@hep.caltech.edu (S. Xie)

particle with a precision of $20 - 30$ ps can effectively reduce the impact of pileup by a factor of 5 to 10.

Highly granular calorimeters based on silicon sensors as the active material have been the focus of recent interest [2, 3], due to radiation hardness considerations as well as maturity of the silicon sensor technology. In this article, we present results of studies of a similar sampling calorimeter prototype using Cadmium-Telluride (CdTe) sensors as the active material. CdTe has been studied extensively in the context of thin film solar cells and has become a mature and wide-spread technology [4]. It is also widely used as a radiation detector for nuclear spectroscopy, and as a sensor for photons in the X-ray range due to its high quantum efficiency in this part of the spectrum [5–8]. This feature is of particular interest in the context of its use in calorimetry because it would enhance the sensitivity to secondary particles in the keV range, a significant component of the electromagnetic shower. Conventional prototypes using silicon sensors have limited sensitive to photons in this energy range. CdTe sensors are available with thicknesses of several mm which will further enhance the efficiency for X-ray photons. Therefore, the first study of electromagnetic showers using CdTe sensors has the potential to yield new insight into the behavior of secondary particles produced within an electromagnetic shower with energies in the keV range, and has the potential to yield an improvement on the energy measurement due to the additional contribution of the higher energy X-ray photons to which previous calorimeters were not sensitive.

The recent interest on precision timing has resulted in new studies of the timing properties of silicon sensors. These studies have found a time resolution at 20 ps level, provided a sufficiently large signal size in a variety of applications ranging from calorimetery [9] to charged particle detectors [10]. The signal formation process in CdTe sensors are very similar to the process in silicon and has similar potential to yield precise timestamps.

In this article, we study the signal response of the CdTe sensor to electromagnetic showers of varying energies and at different shower depths. We also study the timing performance of the CdTe sensors for electromagnetic showers.

2. Cadmium Telluride Sensor

The semi-conducting properties of Cadmium-Telluride has been studied since many decades [4], particularly in the the context of using the material in photovoltaic applications. Cadmium-Telluride sensors are also widely used in X-ray detectors [5, 7, 8]. They have also been investigated for synchrotron radiation detectors in accelerator technology [11], and for three dimensional tracking for neutrinoless double-beta decay [12]. In our previous studies [9, 13–18] we have demonstrated that increasing the primary sensor signal is crucial to achieve good timing resolutions. Cadmium-Telluride features a significantly larger efficiency for detecting photons in the $10 - 100$ keV energy range compared to silicon sensors. The higher atomic number of Cadmium and Tellurium, averaging to 48.52 for the compound bulk material, results in a higher interaction cross section for photons in this energy range. Photons with such energies are abundant in electromagnetic showers [19]. Furthermore, CdTe sensor are available with thicknesses of 1 mm and more. The path-length of the charged shower particles in the sensor material scales accordingly, resulting in a larger primary signal. The higher density of CdTe compared to Si also increases the energy loss of charged particles. A minimal ionizing particle will create about 50k electrons in 300 μm of CdTe, compared to 30k electrons for a Si sensor

[20]. Our measurements were conducted with a CdTe Schottky type diode purchased from Acrorad [21]. It is 1 cm^2 in transverse size and 1 mm thick. It was operated at a bias voltage of 700 V and the dark current was between 3 nA and 6 nA depending on the environmental conditions in the test beam experimental zones. The sensor was placed in a box made of 0.3 mm thick copper sheets. A photograph of the sensor and the copper box enclosing it is shown in Figure 1.

Figure 1: Left: CdTe sensor used for the measurements. The sensor is a Schottky type diode with a transverse size of 1 cm^2 and a thickness of 1 mm. The baseplate is is biased at 700 V. On the front-left corner of the sensor, the wire bond connection to the metalized top layer of the sensor can be seen. On the back-right corner, the wirebond connection to the baseplate can be seen. Right: A photograph of the copper box enclosing the CdTe sensor.

The electrical circuit shown in Fig. 2 was used to connect to the sensor to the bias voltage with a standard high voltage cable and the readout electronics using a SMA cable with a feed through penetrating the copper box.

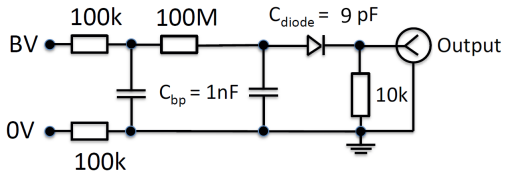

Figure 2: Schematic diagram of the circuit used to polarize and read out the CdTe sensor. The circuit and the sensor are enclosed inside a copper box.

3. Test-beam Setup and Experimental Apparatus

We performed the measurements at the H2 beamline of the CERN North-Area test-beam facility and the T9 beamline of the CERN East-Area testbeam facility. They provide electron beams from the Proton Synchrotron (PS) and Super Proton Synchrotron (SPS) of energies ranging from 2 GeV to 200 GeV. The beams are composed of a mixture of electrons and pions. The electron fraction in the beam at H2 is typically larger than 75% while at T9 it is typically about 10%.

Trigger counters made of photomultipliers coupled to 4 cm $\times$ 4 cm plastic scintillators are used to initiate the read out of the data acquisition (DAQ) system. The DAQ system

uses a CAEN V1742 switched capactor digitizer based on the DRS4 chip [22]. Wire chambers are used to measure the position of each incident beam particle in the plane transverse to the beamline. A stack of lead or tungsten absorbers of different thicknesses are placed about 5 mm in front of the CdTe sensor, which is enclosed within a copper box. We amplified the size of the signals from the CdTe sensor using a Hamamatsu C5594 amplifier [23] with a bandwidth of 1.5 GHz and providing a voltage gain of 36 dB. A 10 dB attenuator was used to attenuate the input signal to the amplifier for beam energies of 50 GeV and above to adjust the CdTe signal to the dynamic range of the amplifier. A micro-channel plate photomultiplier (MCP-PMT) detector is used to provide a very precise reference timestamp. At the T9 beamline, a Hamamatsu R3809U MCP-PMT [24] is placed just upstream of the absorber material. At the H2 beamline a Photek 240 MCP-PMT [25] is used, which contains a significant amount of absorber material (about 1.8 radiation lengths), and is therefore placed just downstream of the CdTe sensor to avoid inducing an early electromagnetic shower. The precision of the time measurement for both types of MCP-PMTs is less than 10 ps [13, 14]. As the purity of the electron beam at the T9 beamline is significantly lower than at the H2 beamline, we use a LYSO crystal optically coupled to an MCP-PMT as a means of discriminating the electrons from the pions in the beam. The entire setup of absorber, reference counter and CdTe sensor box is housed in an aluminum box to provide further shielding against environmental noise. The schematic diagrams of the experimental setups at H2 and T9 are shown in Figure 3, and a photograph of the contents of the aluminum box for the setup at T9 is shown in Figure 4.

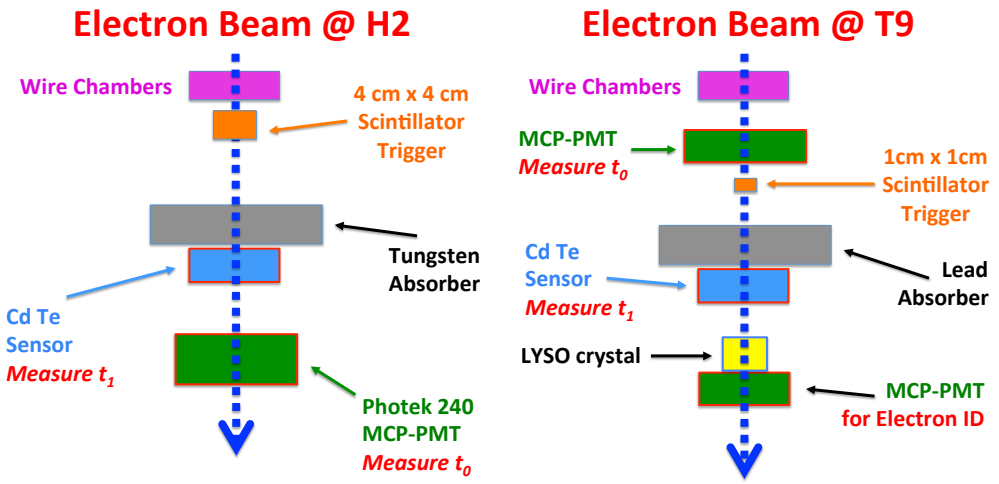

Figure 3: Schematic diagrams of the test-beam setups at H2 (left) and T9 (right) are shown. The timestamps t_0 and t_1 are defined in Section 4.

The horizontal and vertical position measurements from the wire chamber are used to determine the location of the CdTe sensor relative to the beam and to align the beam. In Figure 5, we show the average amplitude measured in the CdTe sensor as a function of the horizontal and vertical positions as measured by the wire chamber. Based on these plots, we can restrict our measurements to those electrons whose impact point is close

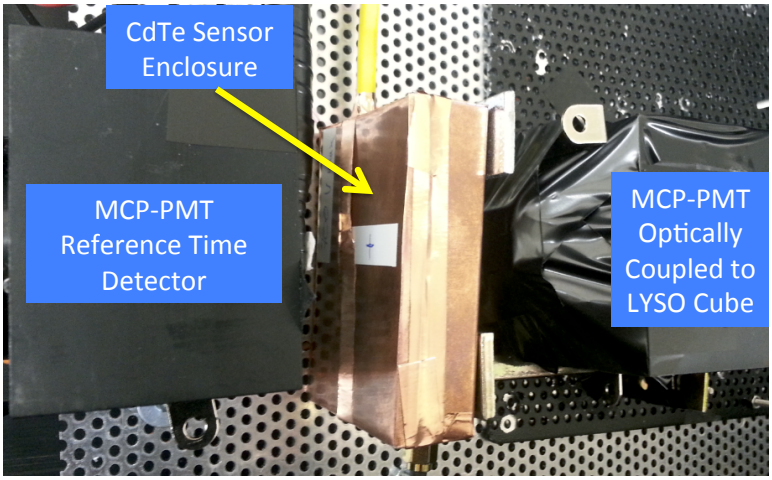

Figure 4: Photograph of the setup used in the T9 beam line. The reference timing MCP-PMT is located on the leftmost region of the photo, followed to the right by a scintillator counter, the copper box enclosing the CdTe sensor and an MCP-PMT optically coupled to a LYSO cube. The lead absorber is not present in the photo and was later inserted in front of the copper box.

to the center of the CdTe sensor.

4. Event Reconstruction and Selection

All signals are recorded by the CAEN V1742 digitizer with a sampling time of 200 ps. The baseline pedestal for each channel is determined using the time samples outside of the signal window, and is subsequently subtracted from the signal pulses. An example of a recorded signal waveform in the CdTe sensor for an electromagnetic shower from a 100 GeV electron is shown in Figure 6. We did not observe an obvious energy dependency of the pulse shapes on the particle energy. The pulses feature two components, an initial faster one lasting about 10 ns followed by a component extending slightly beyond the 200 ns time windown of our readout system. The drift velocity of electrons in CdTe is know to be much higher than for the holes [26], which may cause such a pulse shape. Using randomly triggered data, we measured the RMS of the noise for the channel reading out the CdTe sensor after the amplifier to be about 1.3 mV.

The total charge collected in each channel is obtained by computing the integral of the pulse waveform over the full 200 ns range recorded by the digitizer. The timestamp for each signal is reconstructed by fitting the pulse waveform with an appropriate functional form. For signal pulses from the MCP-PMTs, used as reference timers, we fit a Gaussian function to a 1.5 ns window around the peak of the pulse and extract the timestamp t_0 as the mean parameter of the Gaussian function. For signal pulses from the CdTe sensor, we fit a linear function to time sample points between 10% and 60% of the pulse maximum and the timestamp t_1 is assigned as the time at which the fitted linear function rises to 30% of the pulse maximum. More details of the timestamp reconstruction can be found in reference [13].

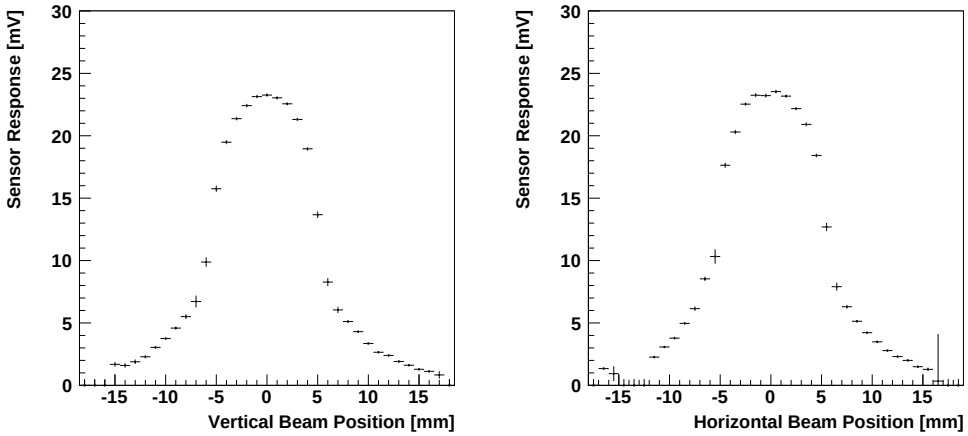

Figure 5: The average amplitude measured in the CdTe sensor is plotted as a function of the horizontal and vertical positions of the beam particle as measured by the wire chamber. The measurement shown was performed with electrons of 100 GeV and 6 X_0 of absorber.

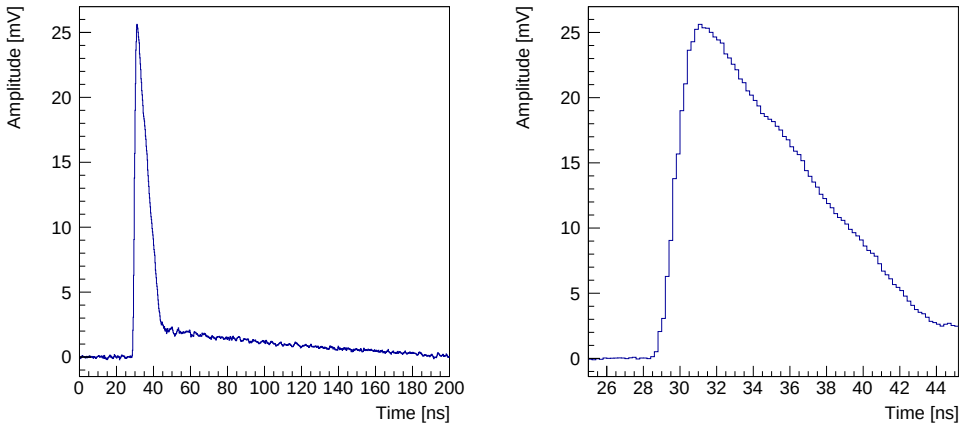

Figure 6: Examples of signal pulse in the CdTe sensor for electrons with energies of 100 GeV. The signal pulse shown was recorded by the CAEN V1742 digitizer after a 10 dB attenuator and a 36 dB fast amplifier. Right: Zoom in of the example pulse.

For the measurements performed at the H2 beamline, based on the results shown in Figure 5 we select events for which the incident beam particle lies within a region of size 3 mm by 3 mm about the center of the sensor. For the measurements performed at the T9 beamline, the resolution of the wire chamber measurement was insufficient to make this requirement. We also require that the signal in the reference MCP-PMT detector has an amplitude larger than 25 mV. For data collected at the H2 beamline, the MCP-PMT detector is located behind the absorbers and can discriminate between electrons that shower in the absorber material and pions that do not. We require that the signal amplitude in the MCP-PMT detector is larger than 500 mV to select a pure sample of electrons. For data collected at the T9 beamline, the electron selection is performed using the LYSO scintillating crystal placed behind the absorber material and the CdTe sensor, as shown in Figure 3. The electromagnetic shower particles produce scintillation light in the LYSO crystal and are read out by an MCP-PMT. We require that the signal amplitude in the MCP-PMT coupled to the LYSO crystal is larger than 800 mV to select a sample of pure electrons. Furthermore, as the precision of the beam particle position measured by the wire chambers at the T9 beamline is relatively poor, we also require large signals in the 1 cm $\times$ 1 cm scintillator trigger counter, with amplitude above 150 mV, to constrain the beam to a smaller geometric region.

5. Calorimetric Measurements

To obtain a preliminary characterization of the calorimetric performance of the CdTe sensors, we measure the total charge collected out of the CdTe sensor for various incident electron beam energies. Examples of the charge distributions are shown in Figure 7 for 2 GeV and 100 GeV electrons. For electrons with energy between 2 GeV and 7 GeV, the sensor was placed after 2 radiation lengths of lead absorber, and for electrons with energy above 50 GeV, the sensor was placed after approximately 6 radiation lengths of three alternating layers of tungsten and lead.

We plot the mean collected charge as a function of the incident beam energy in Figure 8 and observe that the signal size scales up with increasing beam energy. The resolution is measured as the width parameter of a Gaussian fit to the charge distribution and is shown by the green bars. The measured resolution ranges from about 80% for electrons in the range of a few GeV to about 18% for electrons with an energy of 100 GeV. The measurement at 100 GeV was made using events where the incident electron impinged on a 3 $\times$ 3 mm area in the center of the sensor. The same fiducial cut was not applied for the data taken at the T9 beamline as the position measurement resolution was insufficient. These resolution measurements are encouraging given that they are performed using only a single layer sample covering a relatively small transverse geometric area. In future studies, we intend to improve the characterization of the calorimetric performance by completing measurements of the longitudinal shower profile and to instrument a larger transverse area to improve the transverse shower containment.

6. Timing Measurements

We characterize the timing performance of the CdTe sensor by measuring the timestamps relative to the MCP-PMT device used as a reference timer. An example of the

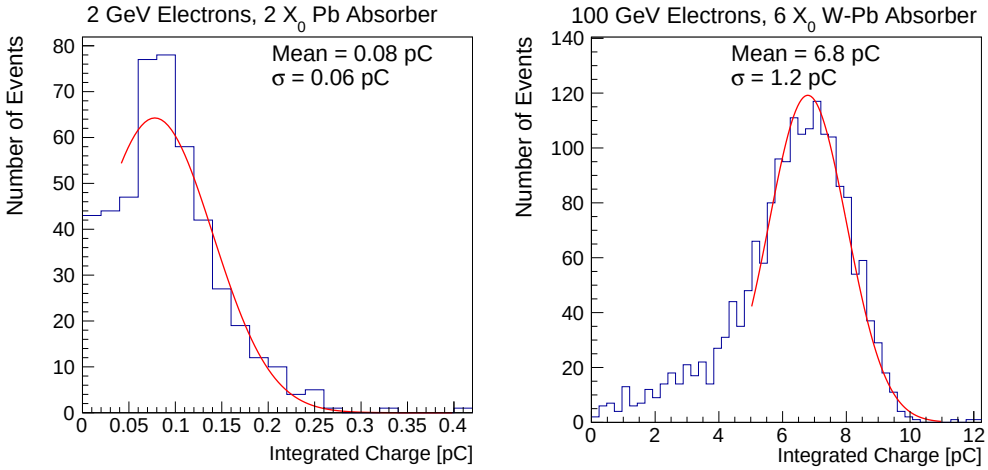

Figure 7: Distribution of total charge collected in the CdTe sensor for a 2 GeV electron after 2 X_0 of lead absorber (left) and a 100 GeV electron after 6 X_0 of tungsten and lead absorber (right). The plot to the right as a fiducial cut with respect to the center of the sensor of 3 × 3 mm applied to the incidenting electrons.

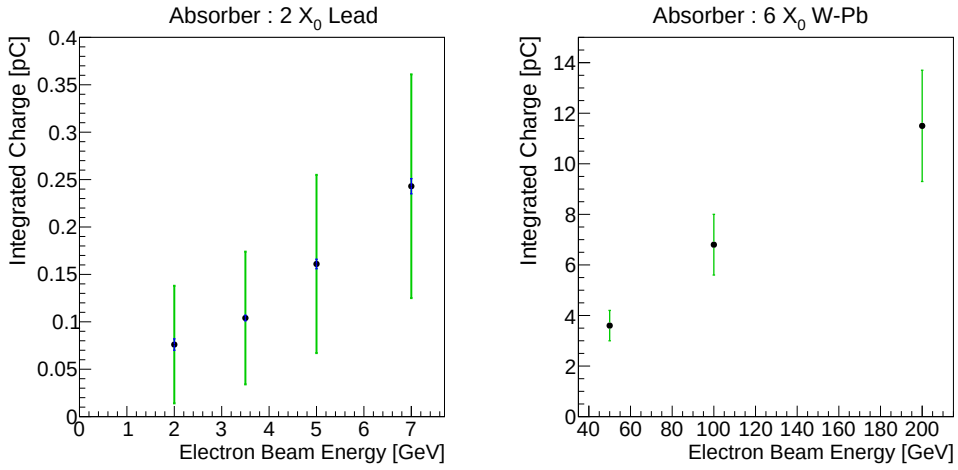

Figure 8: The mean charge collected in the CdTe sensor is plotted as a function of the electron beam energy. Left: Measurements performed at the T9 beamline with 2 X_0 of lead absorber placed directly in front of the CeTe sensor. Right: Measurements performed at the H2 beamline with 6 X_0 of tungsten absorber placed directly in front of the CeTe sensor. The blue bars show the uncertainty on the mean integrated charge extracted from the Gaussian fit to the charge distribution, while the green bars show the measured resolution. The red line is a linear fit to each set of measured data.

distribution of the timestamp measurement for 100 GeV electrons after 6 X_0 of absorber material is shown in Figure 9. We extract the time measurement resolution from this distribution as the width parameter of a Gaussian fit. In Figure 10 we show the measured time resolution as a function of the beam energy. For beam energies below 50 GeV, the time resolution improves with increasing signal size as expected based on the increasing signal-to-noise ratio. However, above 100 GeV, the time resolution no longer improves with increasing signal size, which points towards some systematic limitation. We study a number of such factors in Section 6.1 below.

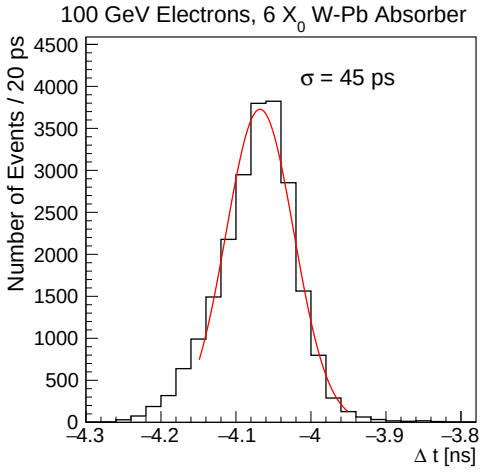

Figure 9: Distribution of the timestamp measurement in the CdTe sensor for a 100 GeV electron after 6 X_0 of tungsten and lead absorber.

To further characterize the timing performance of the CdTe signals, we measure the risetime, defined as the time for the signal to rise from 10% to 90% of its maximum amplitude, for various electron beam energies. The distribution of risetime for 100 GeV electrons and the measured risetime as a function of the beam energy are shown on the left and right of Figure 11 respectively. We observe a risetime of around 1.3 ns that does not vary significantly with the beam energy.

6.1. Studies of Systematic Limitations on Time Resolution

One of the major systematic effects that have been observed in past timing studies [13–15] is the dependence of the time measurement on the amplitude of the signal. On the left of Figure 12, we show the dependence of the timestamp measurement on the amplitude of the signal, and observe a mild dependance on amplitude, which we correct for in subsequent figures. On the right of Figure 12, we show the measured time resolution as a function of the signal amplitude and we observe a clear improvement in the resolution with increasing signal amplitudes up to 0.5 V. In this region, the impact of the signal-to-noise ratio is still the dominant factor for the time resolution.

We also study the dependence of the timestamp measurement as a function of the geometric position of the incident beam particle as measured by the wire chambers in

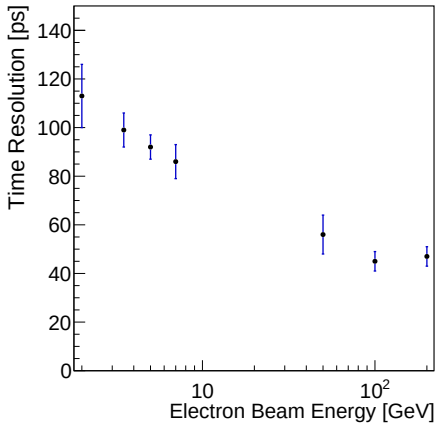

Figure 10: The measured time resolution of the CdTe sensor is plotted as a function of the electron beam energy.

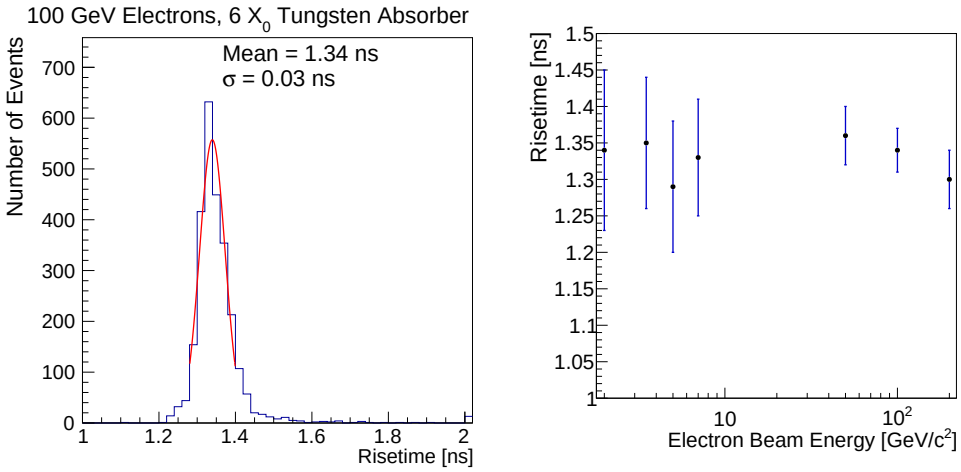

Figure 11: Left: Distribution of risetime of the CdTe signal for 100 GeV electrons. Right: Risetime of the CdTe signal is plotted as a function of the incident beam energy.

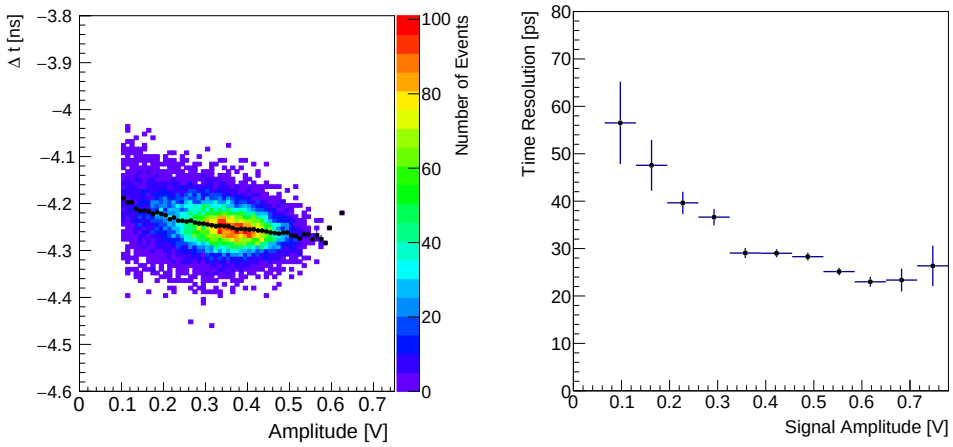

Figure 12: Left: The distribution of the signal amplitude in the CdTe sensor and the time measured in the CdTe sensor relative to the Photek reference detector is shown in the color scale. This data is from a 100 GeV electron beam after 6 X_0 absorber. The mean value of the time measured in the CdTe sensor as a function of the signal amplitude is shown in the black points. Right: The time resolution is measured as a function of the signal amplitude after correction for amplitude non-linearity.

Figure 13. A relatively large and linear dependence is observed, and this position non-uniformity of the time response adds significantly to the time resolution (about 37 ps). Performing a correction for this non-uniformity improves the time resolution from 45 ps to 25 ps for events with 100 GeV electrons. The distribution of timestamps after correcting for the geometric position is shown in Figure 14. The measured time resolution, after correction for the position non-uniformity, has a mild dependence on the beam particle position and is shown in Figure 15. Combining the time resolution dependence on the horizontal and vertical beam positions, we measure the time resolution as a function of the planar distance between the beam position and the location of the back wire bond on the CdTe sensor, and observe a more clear dependence shown in Figure 16. More detailed studies are necessary to derive a better understanding of this effect. It will be crucial for any precision timing device using planar semi-conductor sensors to study the uniformity of the response to achieve an optimal performance.

7. Discussion and Summary

In this article, we describe the first measurement of high energy electromagnetic showers using Cadmium-Telluride sensors. These initial results are encouraging and motivate future work on more detailed comparisons with simulation and more detailed measurements of transverse and longitudinal shower profiles.

We have measured the rise time for signals in the Schottky type CdTe sensor diode to be about 1.3 ns which makes them suitable as devices for precision timing applications. The large ionization signal yield we achieve with a 1 mm thick sensor is equally favorable for precision timing applications. We observe dependencies of the measured time on the geometric position of the beam particle impact point on the sensor, which may indicate

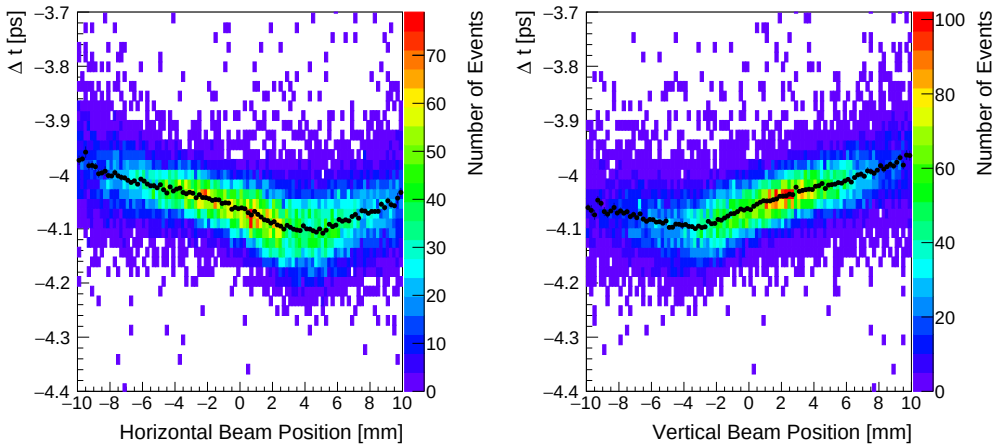

Figure 13: The distribution of the beam particle position measured by the wire chamber and the time measured in the CdTe sensor relative to the Photek reference detector is shown in the color scale. The mean value of the time measured in the CdTe sensor as a function of the beam particle position is shown in the black points. There is a dependence of the time difference on the impact point on the CdTe sensor which corresponds to about 100 ps across the CdTe sensor.

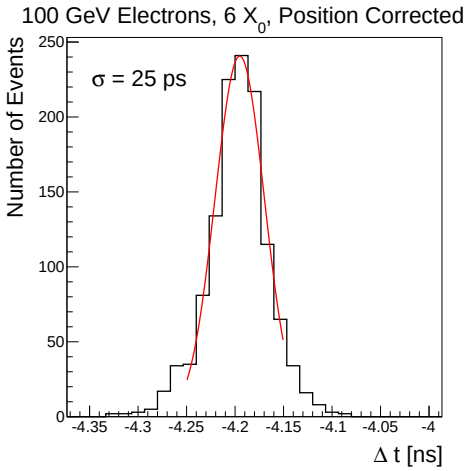

Figure 14: Distribution of the timestamp measurement corrected for the geometric position non-uniformity in the CdTe sensor for a 100 GeV electron after 6 X_0 of tungsten absorber.

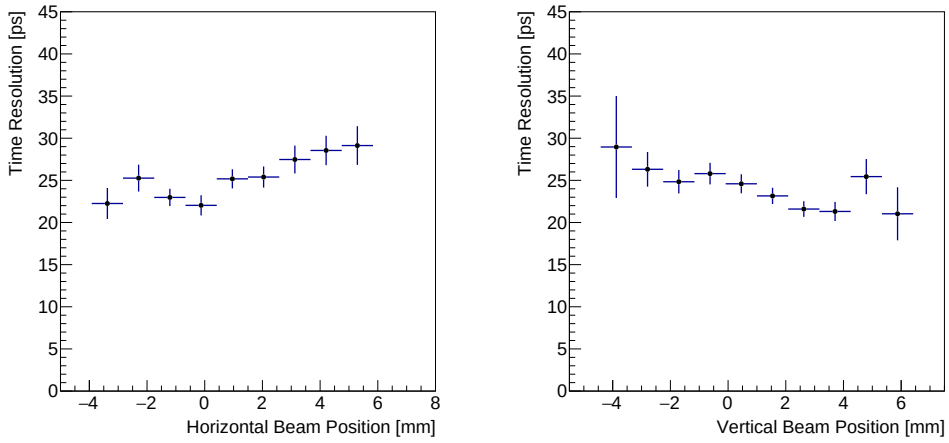

Figure 15: The time resolution is measured as a function of the horizontal (left) and vertical (right) beam position in a 2 mm wide fiducial region around the center of the sensor in the vertical (left) and horizontal (right) directions respectively.

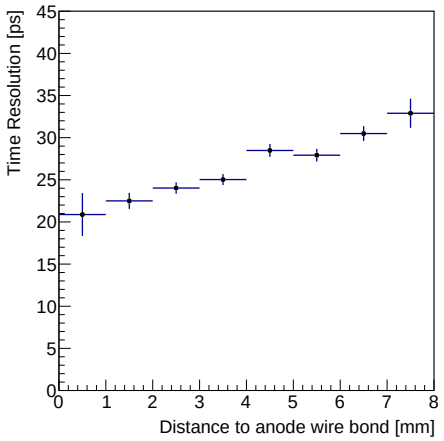

Figure 16: The time resolution is measured as a function of the planar distance of the incident beam particle to the back wire bond location on the sensor. The position non-uniformity of the time response as shown in Fig. 13 has been corrected for. There remains a dependence of the measured resolution across the sensor, reaching 20 ps in the location closest to the back wire bond connection.

differences in the charge collection dynamics. More detailed studies of this aspect are needed and a more optimal design of the connection of the sensor readout is envisioned. Correcting for these dependencies yield time resolutions of 25 ps for a single layer CdTe sensor of transverse area 1 cm $\times$ 1 cm, uniformly sampled by the electromagnetic shower of electrons with energy above 100 GeV after 6 radiation lengths of tungsten and lead absorber. In the most favorable region of the sensor we observe time resolutions as low as 20 ps. These initial results are encouraging and motivate further in-depth studies in the future.

8. Acknowledgements

Supported by funding from California Institute of Technology High Energy Physics under Contract DE-SC0011925 with the United States Department of Energy. We thank the CERN testbeam facilities personnel for excellent beam conditions during our test-beam time. We also thank Paolo Meridiani and Francesco Micheli for their kind assistance on the setup of the DAQ system.

References

[1] A. Bornheim, "On the Usage of Precision Timing Detectors in High Rate and High Pileup Environments," *PoS(Vertex2016)044*, 2016.

[2] C. Adloff *et al.*, "Response of the CALICE Si-W electromagnetic calorimeter physics prototype to electrons," *Nucl. Instrum. Meth. A*, vol. 608, pp. 372–383, 2009.

[3] J. Butler, D. Contardo, M. Klute, J. Mans, and L. Silvestris, "Technical Proposal for the Phase-II Upgrade of the CMS Detector," Tech. Rep. CERN-LHCC-2015-010. LHCC-P-008, CERN, Geneva, Jun 2015.

[4] D. A. Jenny and R. H. Bube, "Semiconducting cadmium telluride," *Phys. Rev.*, vol. 96, pp. 1190–1191, Dec 1954.

[5] P. Capper, *Properties of Narrow Gap Cadmium-Based Compounds*. INSPEC, 1994.

[6] K. Zanio, "Purification of CdTe from, tellurium-rich solutions," *Journal of Electronic Materials*, vol. 3, no. 2, pp. 327–351, 1973.

[7] A. R.Triboulet, Y.Marfaing and P.Siffert, "Undoped highresistivity cadmium telluride for nuclear radiation detectors," *Journal of Applied Physics*, vol. 45, no. 6, p. 2759, 1974.

[8] F.V.Wald and G.Entine, "Crystal growth of CdTe for γ-ray detectors," *Nucl. Instrum. Meth. A*, vol. 150, no. 1, pp. 13 – 23, 1978.

[9] A. Apresyan, G. Bolla, A. Bornheim, H. Kim, S. Los, C. Pena, E. Ramberg, A. Ronzhin, M. Spiropulu, and S. Xie, "Test beam studies of silicon timing for use in calorimetry," *Nucl. Instrum. Meth. A*, vol. 825, pp. 62 – 68, 2016.

[10] H. F.-W. Sadrozinski, S. Ely, V. Fadeyev, Z. Galloway, J. Ngo, C. Parker, B. Petersen, A. Seiden, A. Zatserklyaniy, N. Cartiglia, F. Marchetto, M. Bruzzi, R. Mori, M. Scaringella, and A. Vinattieri, "Ultra-fast silicon detectors," *Nucl. Instrum. Meth. A*, vol. 730, pp. 226 – 231, 2013.

[11] E. Rossa, C. Bovet, D. Meier, H. Schmickler, L. Verger, F. Mongellaz, and R. G., "CdTe Photoconductors for LHC Luminosity Monitoring," *CERN-SL-2000-068 BI*, 2000.

[12] M. Filipenko, T. Gleixner, G. Anton, and T. Michel, "3D particle track reconstruction in a single layer cadmium-telluride hybrid active pixel detector," *Eur. Phys. J.*, vol. C74, no. 8, p. 3013, 2014.

[13] D. Anderson, A. Apresyan, A. Bornheim, J. Duarte, C. Pena, A. Ronzhin, M. Spiropulu, J. Trevor, and S. Xie, "On Timing Properties of LYSO-Based Calorimeters," *Nucl. Instrum. Meth. A*, vol. 794, pp. 7–14, 2015.

[14] A. Ronzhin, S. Los, E. Ramberg, A. Apresyan, S. Xie, M. Spiropulu, and H. Kim, "Study of the timing performance of micro channel plate photomultiplier for use as an active layer in shower maximum detector," *Nucl. Instrum. Meth.*, vol. 795, pp. 288–292, 2015.

[15] A. Ronzhin, S. Los, E. Ramberg, A. Apresyan, S. Xie, M. Spiropulu, and H. Kim, "Direct tests of micro channel plates as the active element of a new shower maximum detector," *Nucl. Instrum. Meth. A*, vol. 795, pp. 52 – 57, 2015.

[16] A.Apresyan, S.Los, C.Pena, F.Presutti, A.Ronzhin, M.Spiropulu, and S.Xie, "Direct tests of a pixelated microchannel plate as the active element of a shower maximum detector," *Nucl. Instrum. Meth. A*, vol. 828, pp. 1 – 7, 2016.

[17] D. Anderson, A. Apresyan, A. Bornheim, J. Duarte, C. Pena, A. Ronzhin, M. Spiropulu, J. Trevor, and S. Xie, "Precision Timing Calorimeter for High Energy Physics," *IEEE Trans. Nucl. Sci.*, vol. 63, no. 2, pp. 591–595, 2016.

[18] D. Anderson *et al.*, "Precision Timing Measurements for High Energy Photons," *Nucl. Instrum. Meth.*, vol. A787, pp. 94–97, 2015.

[19] R. Wigmans, *Calorimetry - Energy Measurement in Particle Phyiscs.* Oxford University Press, 2000.

[20] E. Rossa, E. Gschwendtner, M. Placidi, H. Schmickler, A. Brambilla, F. Mongellaz, L. Verger, V. Cindro, M. Mikuz, and P. Moritz, "Fast Polycrystalline-CdTe Detector for LHC Luminosity Measurements," *CERN-SL-2002-002 BI*, 2002.

[21] "Acrorad Co., Ltd.," *http://www.acrorad.co.jp/.*

[22] S. Ritt, R. Dinapoli, and U. Hartmann, "Application of the DRS chip for fast waveform digitizing," *NIM* **A** *623 (2010) 486-488.*

[23] `http://http://www.hamamatsu.com/resources/pdf/etd/C5594_TACC1068E.pdf`.

[24] `http://www.hamamatsu.com/resources/pdf/etd/R3809U-50_TPMH1067E09.pdf`.

[25] `http://www.photek.com/pdf/datasheets/detectors/DS006_Photomultipliers.pdf`.

[26] J. Fink, P. Lodomez, H. Kruer, H. Pernegger, P. Weilhammer, and N. Wermes, "TCT characterization of different semiconductor materials for particle detection," *Nucl. Instrum. Meth. A*, vol. 565, no. 1, pp. 227 – 233, 2006.